Desalination and Water Treatment
www.deswater.com

doi: 10.1080/19443994.2015.1050700

57 (2016) 12375–12384
June

Taylor & Francis
Taylor & Francis Group

Adsorptive removal of bisphenol-A by rice husk ash and granular activated carbon—A comparative study

P. Sudhakar, Indra Deo Mall*, Vimal Chandra Srivastava

Department of Chemical Engineering, Indian Institute of Technology Roorkee, Roorkee 247667, Uttarakhand, India,
Tel. +91 1332 285319; Fax: +91 1332 276535; emails: sudhakarpabbu58@gmail.com (P. Sudhakar), id_mall2000@yahoo.co.in
(I.D. Mall), vimalcsr@yahoo.co.in, vimalfch@iitr.ac.in (V.C. Srivastava)

Received 24 June 2014; Accepted 29 April 2015

ABSTRACT

Present study was performed so as to compare adsorptive removal efficiencies of low-cost adsorbent rice husk ash (RHA) and commercial granular activated carbon (GAC) for the removal of bisphenol-A (BPA), an endocrine disrupting chemical, from aqueous solution. Effect of variables such as initial concentration (C_0), adsorbent dose (m), temperature (T), pH, and time (t) were studied. Optimized values at $C_0 = 100$ mg/L were found to be: $m = 30$ g/L, $t = 3$ h for RHA whereas for GAC, optimum values were: $m = 20$ g/L and $t = 2$ h. Pseudo-second-order model best represented the adsorption kinetic data; and Freundlich and Temkin models best fitted the isotherm data. The adsorption of BPA onto GAC and RHA was found to be endothermic in nature. Value of change in entropy and enthalpy for BPA adsorption onto RHA was found to be: 21.38 J/mol K and 0.335 kJ/mol, respectively. Respective values for BPA adsorption onto GAC were found to be: 29.6 J/mol K and 4.03 kJ/mol, respectively.

Keywords: Bisphenol A; Rice husk ash; Granular activated carbon; Adsorption kinetics; Adsorption isotherm

1. Introduction

In the past few years, research on the endocrine disrupting chemicals (EDCs) such as bisphenol-A (BPA) [2, 2-bis (4-hydroxyphenyl) propane] has increased with great interest owing to their estrogenic, anti-estrogenic, and anti-androgenic nature which leads to the potential damage the endocrine systems of human beings and other living organisms. BPA is mainly used in the manufacturing of resins and polycarbonate plastics. It can enter into water bodies while manufacturing plastic products, leaching from plastic products, from landfill sites, and many other routes causing contamination of ground water, surface water, etc. [1].

Many studies have been reported on adsorptive removal of BPA using various types of adsorbents such as mesoporous carbon, CMK-3 with high surface area of 920 m^2/g [1], acetylaniline modified hyper-cross-linked polymeric [2], polyethersulfone organophili montmorillonite hybrid particles [3], sediments [4], carbonaceous materials [5], hyper-cross-linked, and animated adsorbents [6]. Sewage waste (activated sludge and inactivated sludge) converted into adsorbent material [7] and membranes [8] have also been studied for removing BPA.

---

*Corresponding author.

If the adsorbent is readily available and inexpensive, adsorption process is an attractive treatment due to its various advantages such as ease of operation and handling, regeneration, sludge free operation, and economic feasibility [9]. Many natural adsorbents such as chitosan, bark, wood chips, sugarcane, peat, bagasse, rice husk, straw, and activated bamboo are used as adsorbents for the removal of pollutants from the wastewater [10–13]. Activated carbon is one of most popular adsorbent due to its great success, however, it is very expensive and its regeneration increases the cost. Consequently, feasibility of using low-cost adsorbent to remove various pollutants from wastewater has been studied [14]. Rice husk which is obtained as an agriculture waste after separation of paddy in rice mills is used as fuel to produce steam in many industries such as sugar, paper. Particulate collection equipment is used to collect the rice husk ash (RHA) from the stack of rice husk fired boilers. Thus, RHA is available abundantly and almost free of cost.

Aim of this study was to explore the possibility of using RHA as an adsorbent for removing BPA by adsorption from aqueous solution and to compare its performance with that of granular activated carbon (GAC). Effect of the parameters such as initial concentration (C_0), adsorbent dose (m), temperature (T), pH, and time (t) have been studied. Adsorption kinetics of BPA onto RHA and GAC was analyzed using various kinetic models. Experimental data was fitted to the Freundlich, Langmuir, and Temkin isotherm equations to find the best-fit isotherm model. Thermodynamics parameters of the adsorption process have also been determined.

2. Materials and methods

2.1. Adsorbate and adsorbent

RHA was obtained from Triveni sugar mill, Deoband, UP, India whereas GAC was supplied by Zeo Tech Adsorbents Pvt Ltd, New Delhi, India. BPA was supplied by Sisco Reseach Laboratories Pvt Ltd, Mumbai, India. BPA solution was prepared by mixing a 1 g of BPA in 1,000 mL of distilled water to prepare 1,000 mg/L solution.

2.2. Instrumentation

Philips X-ray diffraction (XRD) unit (PW1140/90) with nickel as filter and copper as target was used for the XRD analysis. A constant wavelength of 1.542 Å was used with goniometric speed of 1°/min. LEO 435 VP scanning electron microscope (SEM) was used to analyze morphology of blank and BPA-loaded RHA and GAC. Nicolet Avatar 370 CsI spectrometer was used to obtain FTIR spectra over 4,000–400 cm^{-1} range using KBr pellet technique. Bulk density of RHA and GAC were measured using MAC bulk density meter. HACH DR 5,000 double beam UV–vis spectrometer was used to determine the initial and final concentrations of BPA. Adsorbent surface area was determined by adsorption of liquid N_2 at 77.15 K.

2.3. Batch adsorption study

Each experiment was carried out using 100 mL of known solution of BPA in a conical flask along with known amounts of RHA and GAC. HCl and NaOH solutions were used to adjust the initial pH. BPA containing solution was agitated along with the known amount of adsorbents in an orbital shaker at a constant speed of 150 rpm under controlled temperature. BPA removal percentage was calculated using the following relation:

$$\text{Percentage BPA removal at any time '}t\text{'} = \left(\frac{C_o - C_t}{C_o}\right) \times 100 \tag{1}$$

Uptake of adsorbate at any time "t" was calculated using following relation:

$$q_t(\text{mg/g}) = \left(\frac{C_o - C_t}{m}\right)V \tag{2}$$

where C_0 is initial BPA concentration (mg/L), C_t is the BPA concentration at time t, m is the mass of adsorbent (g), and V is volume of solution (L).

3. Results and discussion

3.1. Characterization of adsorbent

Brunauer Emmett Teller (BET) surface area of RHA and GAC was found to be 21.6 and 137.9 m^2/g, respectively. Srivastava et al. [10] also reported BET surface area of 36.44 m^2/g for RHA. RHA forms during heating of rice husk at higher temperature which causes reduction in carbon content and increase in silicon dioxide proportion in RHA [11]. Low percentage of carbon in RHA causes low surface area of RHA as compared to GAC [12,13].

Bulk density of RHA and GAC was found to be 251 and 638 kg/m^3, respectively. XRD spectra (Fig. 1) of GAC showed the presence of silicon oxide

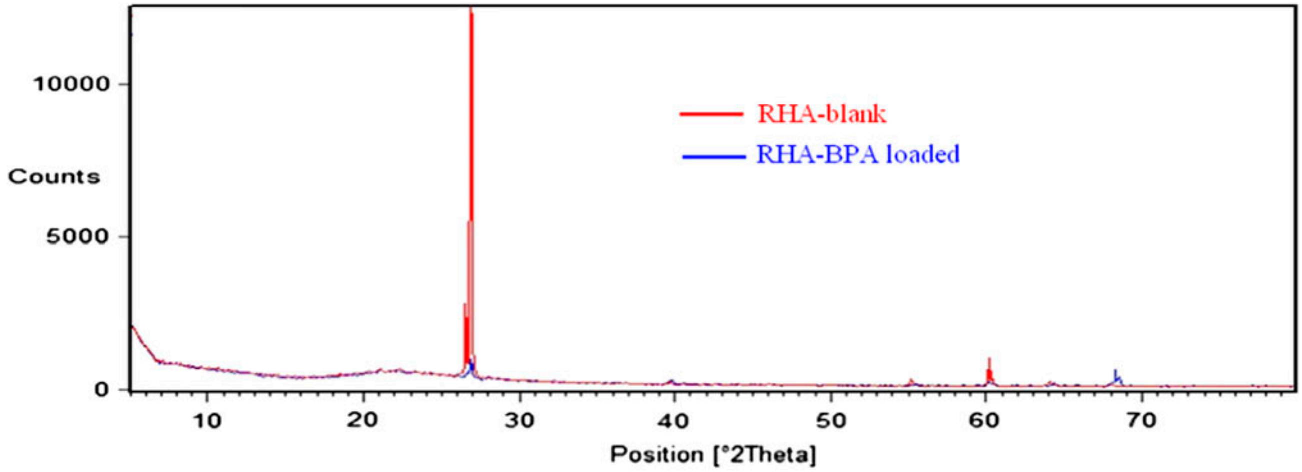

(a) RHA-blank and RHA-BPA loaded

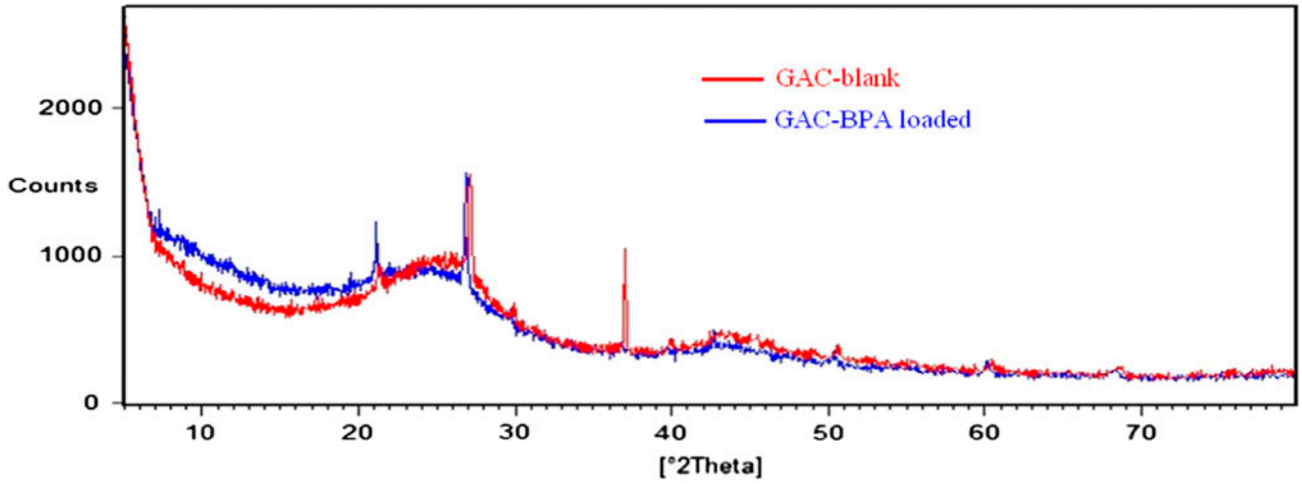

(b) GAC-blank and GAC-BPA loaded

Fig. 1. XRD spectra of blank and BPA-loaded RHA and GAC.

(SiO_2), aluminum oxide hydroxide [$4Al_2O_3.H_2O$], and Fersilicate (FeSi), whereas RHA was found to contain silica (SiO_2) only. Hump in the 2θ range of 15–30° in both GAC and RHA (not clearly visible in RHA because of sharp peaks of ≈13,000 arbitrary units at $2\theta = 28°$) correspond to the presence of silica. It may be seen in Fig. 1 that no significant change in XRD spectra was observed after BPA loading.

Morphology of adsorbents was studied by SEM analysis. SEM images of virgin and BPA-loaded GAC and RHA are shown in Fig. 2. SEM images of RHA show presence of linear fibrous structure with large number of pores and skeleton-like structure. Also, RHA has less number of pores as compared to GAC.

FTIR spectra of the adsorbents are shown in Fig. 3. Broad peak in the range of 3,100–3,700 cm^{-1} was observed in both the adsorbents. These peaks are due to presence of OH groups on the surface of adsorbent [15]. FTIR spectra also shows a light signal corresponding to OH groups bounded to methyl radicals in both the adsorbents. Stretching at the 3,400 cm^{-1} may be due to Si bonded to the OH group of the adsorbed water [16]. Weak and broad peaks in the range of 1,600–1,800 cm^{-1} indicate the presence of CO group stretching from ketones and aldehydes. Peak at 1,600 cm^{-1} may also be due to the conjugated hydro carbon which is bonded to the carbonyl groups. Peak at 1,100 cm^{-1} is due to vibration of CO functional group present in the lactones [17]. Aromatic CH and carboxyl–carbonate structures are indicated by peaks in the range of 1,360–1,420 cm^{-1} [18]. The weak and broad bands do not provide any authentic information about the nature of the surface oxides on RHA and GAC. It may be noted that the FTIR of blank- RHA or GAC are

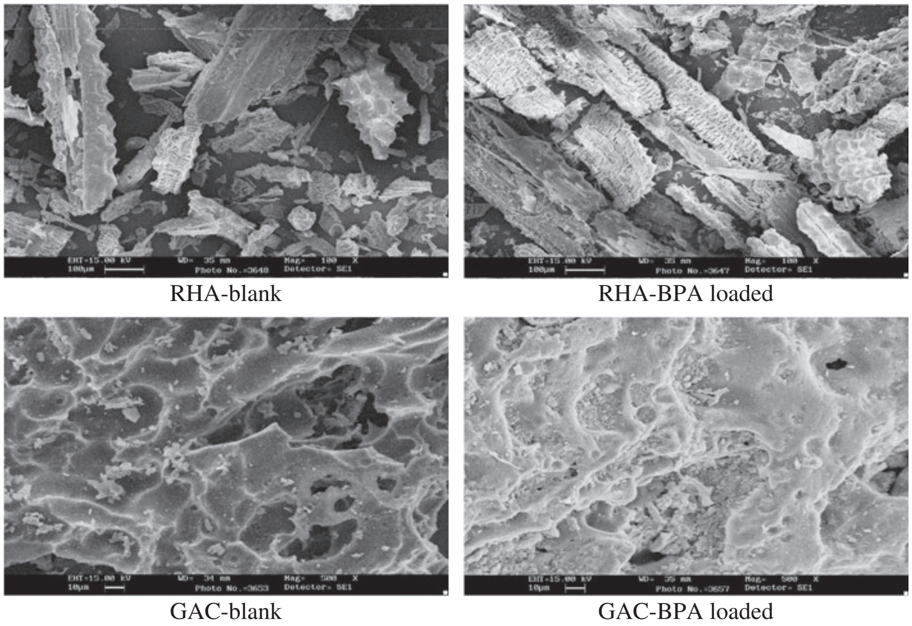
RHA-blank RHA-BPA loaded

GAC-blank GAC-BPA loaded

Fig. 2. SEM of blank and BPA-loaded RHA and GAC.

different, indicating presence of different types of functional groups on the surface of RHA and GAC. FTIR of blank-adsorbent (RHA or GCA) and the BPA-loaded adsorbents are similar, though there is marginal shift in the peaks before and after adsorption indicating that the adsorption process in more physical in nature.

3.2. Effect of adsorbents dosage and pH

The effect of adsorbent dose (*m*) on BPA removal is shown in Fig. 4. The residual concentration of BPA in the solution rapidly decreased with an increase in the m value, which is due to increase in the number of actives adsorption sites at increased *m* [19]. It is clear from Fig. 4 that GAC is more effective than RHA for removal of BPA.

Effect of pH is shown in Fig. 5. Different values of pH ranging from 2 to 12 were taken by adjusting with HCl and NaOH solutions. Results clearly indicate that the removal efficiency was not affected much by change in pH. It may be due to the physical nature of the overall adsorption process as evidenced by the FTIR and thermodynamic analysis (given in later section). Further studies were done at natural pH of BPA solution without any pH adjustment.

3.3. Effect of initial BPA concentration

The effect of C_0 is shown in Fig. 6. It is clearly evident that significant decrease in BPA removal efficiency was observed as the BPA concentration in the solution was increased from 20 to 350 mg/L. At lower BPA concentration, percent removal was high because the numbers of adsorbates molecules competing for the same number of adsorbent sites were less in comparison to at high BPA concentration [20]. Therefore, the residual concentration in case of higher C_0 was high and caused low BPA removal.

3.4. Effect of contact time and kinetics of adsorption

Results shown in Fig. 7 indicate that for a particular BPA concentration, the percent removal of BPA increases with an increase in contact time. For longer treatment time, the adsorbate is able to diffuse longer distance and overcome resistance until equilibrium is achieved. Due to the availability of large number of sites during initial stages, rate of adsorption is high at initial stage. Rapid uptake of adsorbate was seen in first 30 min of adsorption. The initial high rate of removal indicates surface bound sorption, and after sometime, removal rate became less. This can be attributed to long range diffusion of adsorbate into the interior pores of the adsorbent [21]. After sufficient time, the concentration of BPA in aqueous phase and at adsorbent surface comes into equilibrium and thus no further adsorption was observed.

Adsorption process of BPA on RHA and GAC was investigated by frequently used kinetic models namely pseudo-first-order, pseudo-second-order, and

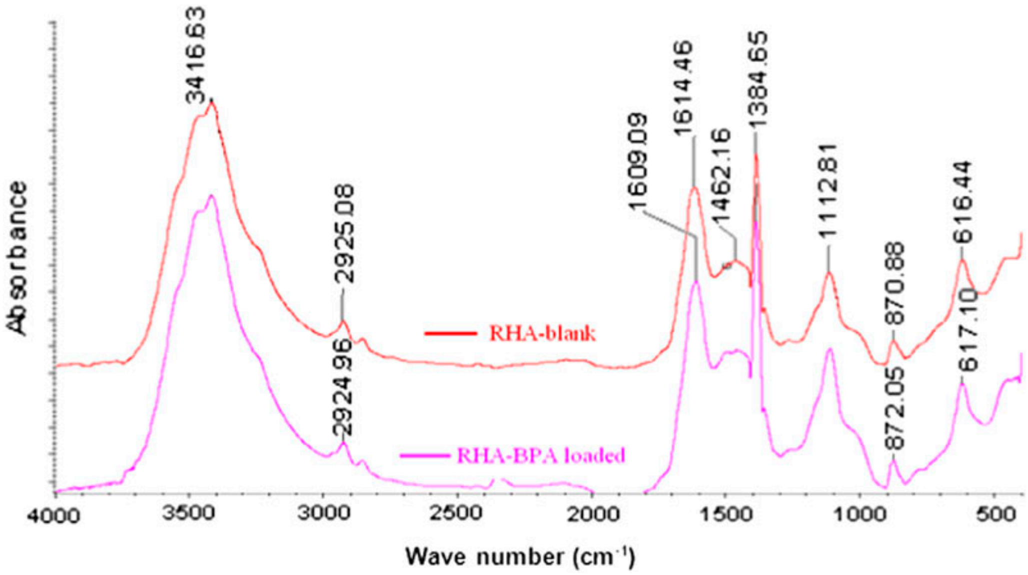

(a) RHA-blank and RHA-BPA loaded

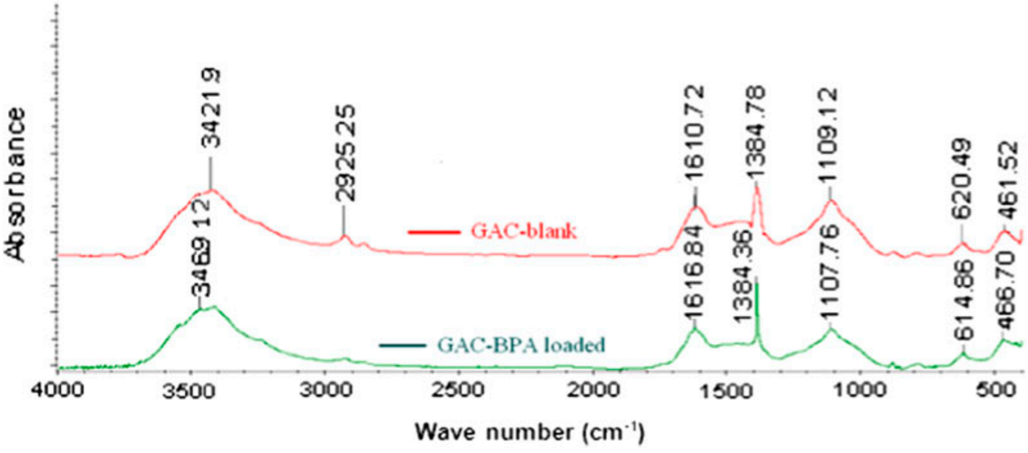

(b) GAC-blank and GAC-BPA loaded

Fig. 3. FTIR spectra of blank and BPA-loaded RHA and GAC.

intraparticle diffusion models. Pseudo-first-order equation is represented in mathematical form as follows:

$$q_t = q_e[1 - \exp(-k_f t)] \tag{3}$$

where q_t is amount of adsorbate adsorb at time t (mg/g), q_e is adsorption capacity at equilibrium (mg/g), and k_f is pseudo-first-order constant. Pseudo-second-order equation is represented in the following form [22]:

$$q_t = \frac{t k_s q_e^2}{1 + t k_s q_e} \tag{4}$$

where k_s is pseudo-second-order rate constant (g/mg min). Initial adsorption rate, h (mg/g min) is defined as

$$h = k_s q_e^2 \tag{5}$$

The best-fit values of kinetic parameters such as k_f, h, q_e, and k_s are shown in Table 1. Coefficient of determination (R^2) values show that the adsorption kinetic data fits best to the pseudo-second-order model for both the adsorbents. It is observed that the h and q_e values of GAC are higher than RHA for the same C_0.

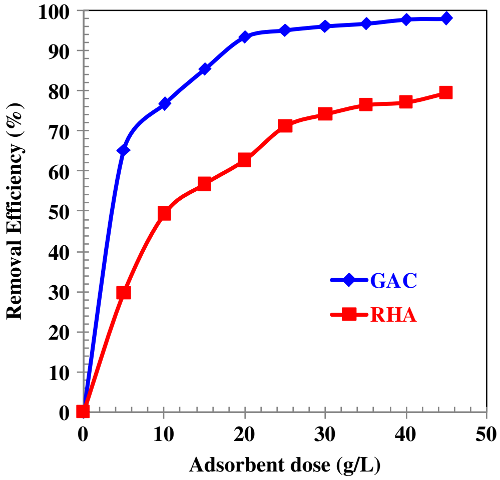

Fig. 4. Effect of adsorbent dose on the removal of BPA by RHA (t = 180 min, pH 6 and T = 30°C, C_0 = 100 mg/L) and GAC (t = 120 min, pH 6 and T = 30°C, C_0 = 100 mg/L).

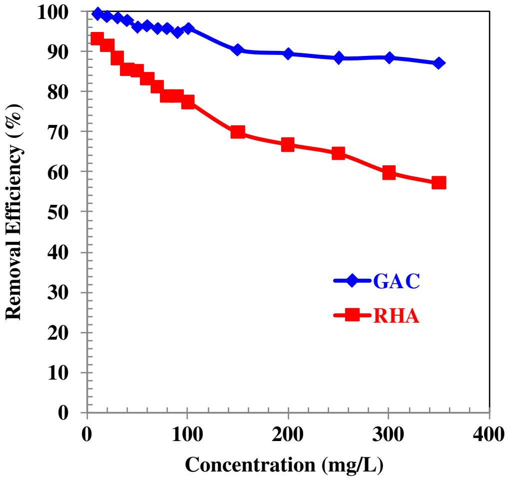

Fig. 6. Effect of initial BPA concentration (C_0) on the removal of BPA by RHA (t = 180 min, pH 6, m = 30 g/L, C_0 = 10–400 mg/L) and GAC (t = 120 min, pH 6, m = 20 g/L, C_0 = 10–400 mg/L).

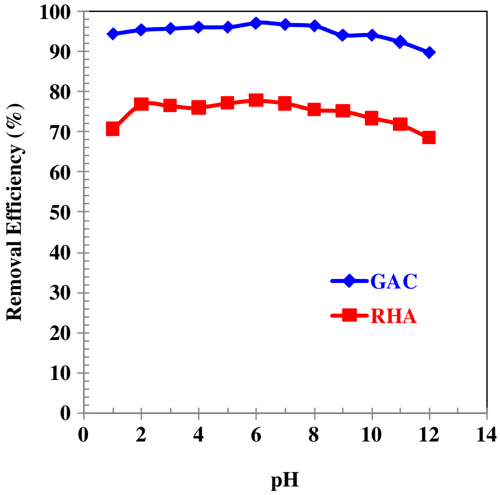

Fig. 5. Effect of pH on the removal of BPA by RHA (t = 180 min, m = 30 g/L, T = 30°C, C_0 = 100 mg/L) and GAC (t = 120 min, m = 20 g/L, T = 30°C, C_0 = 100 mg/L).

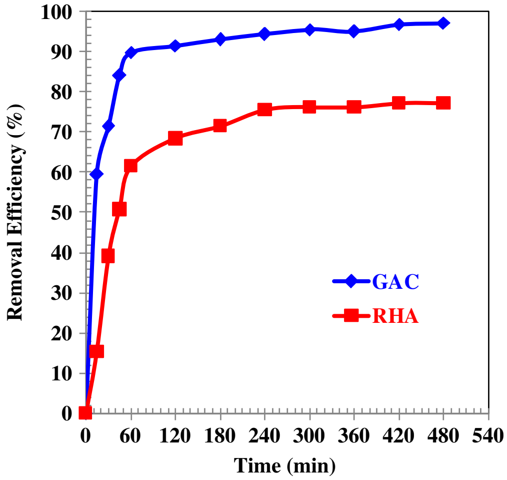

Fig. 7. Effect of contact time on the removal of BPA by RHA (m = 30 g/L, pH 6, T = 30°C, C_0 = 100 mg/L) and GAC (m = 20 g/L, pH 6, T = 30°C, C_0 = 100 mg/L).

3.5. Intraparticle diffusion model/rate controlling

In the adsorption process, the transport of adsorbate from solution to the surface of adsorbent is considered to be completed in following steps: (a) movement of adsorbate from solution to the surface of adsorbate known as film or external diffusion, (b) transfer of adsorbate from boundary layer to surface, (c) diffusion of BPA molecule to the adsorption sites either by pores diffusion process or through solid surface diffusion mechanism, and (d) adsorption of adsorbate at adsorbent sites [23]. Adsorption mechanism of BPA onto RHA and GAC was investigated by intraparticle diffusion model [24]:

$$q_t = k_{\text{id}} t^{1/2} + I \tag{6}$$

where k_{id} is defined as intraparticle diffusion rate constant (mg/g min ½) and I is a constant, which is obtain from the intercept of the plot q_e vs. $t^{0.5}$. Value of I gives an idea about the thickness of the boundary layer. Larger the intercept, greater is the boundary layer effect and slower is the corresponding step.

Table 1
Kinetic parameters for the removal of bisphenol-A by RHA (t = 180 min, m = 30 g/L, T = 303 K) and GAC (t = 120 min, m = 20 g/L, T = 303 K)

Pseudo-first-order						
Adsorbent	q_e (mg/g)	k_f (min^{-1})	R^2			
RHA	3.16	0.0391	0.9931			
GAC	5.41	0.0658	0.994			
Pseudo-second-order						
Adsorbent	q_e (mg/g)	k_s (g/mg min)	h	R^2		
RHA	2.65	0.0242	0.170	0.9981		
GAC	4.88	0.0295	0.68	0.9995		
Intraparticle diffusion						
Adsorbent	$k_{id,1}$ (mg/g min$^{1/2}$)	I_1 (mg/g)	R^2	$k_{id,2}$ (mg/g min$^{1/2}$)	I_2 (mg/g)	R^2
RHA	0.0354	0.058	0.9811	0.0008	2.24	0.7887
GAC	0.034	2.550	0.9797	0.0007	4.5287	0.9124

Fig. 8 shows a plot between q and $t^{0.5}$ at different concentration of BPA for both the adsorbents. The lines in Fig. 8 do not pass through origin leading to the conclusion that there is difference in initial and final rate of adsorption. From the figure, it is evident that the plots are multilinear over the full $t^{0.5}$ range. First sharper portion connecting origin to first point of each line and further two linear portions represent various stages of adsorption [25]. The first linear portion represents macro-pore diffusion or surface diffusion and it can be attributed to gradual equilibrium stage with intraparticle diffusion dominating. Second linear portion represents meso-pore diffusion and in this intraparticle diffusion [26]. Values of $k_{id,1}$, I_1, $k_{id,2}$, and I_2 are shown in Table 1. From the results, it is observed that the value of k_{id} for first linear portion is about six times of second portion which signifies higher rate of adsorption. Due to larger value of intercept for second line, the resistance will be more causing slower rate of adsorption during large phase of removalprocess. From Table 1, it is evident that with increase in concentration, value of k_{id} increases.

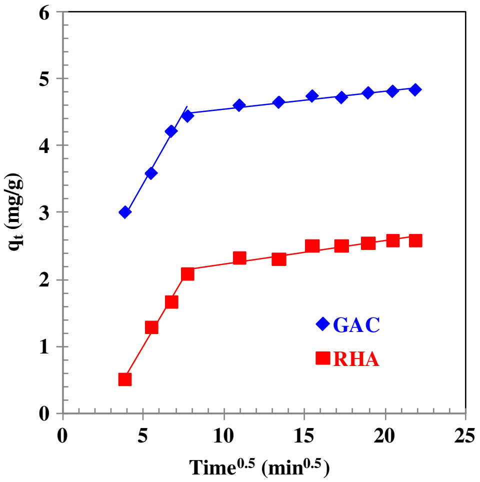

Fig. 8. Webber-Morris plot for BPA removal by RHA and GAC.

3.6. Adsorption isotherm study

Operating temperature in adsorption process affects the equilibrium uptake in various capacities. A plot of q_e vs. C_e for BPA-RHA and BPA-GAC systems is shown in Fig. 9 at various temperatures (15, 30, 45℃). Normally adsorption process is considered as exothermic process, and that the adsorption capacity should decrease with increase in temperature. However, in the present study, contrary to normal observation, adsorption was found to increase with an increase in temperature for both the absorbents. Increase in adsorption capability can be attributed to activation of new sites due to increase in temperature as well as increase in mobility of BPA molecules at high temperature and decrease in retardation force. Diffusivity is positively affected by temperature and it contributes in the enhancement of adsorption capacity of adsorbate with increase in temperature provided that adsorption process is controlled by diffusion process, which is the case as established in earlier sections. Along with intraparticle diffusion, adsorption is also controlled by surface diffusion and diffusion resistance can be neglected if process is continued for sufficient contact time [19,20].

Relation between the amount of adsorbate adsorbed on the adsorbent and the concentration in

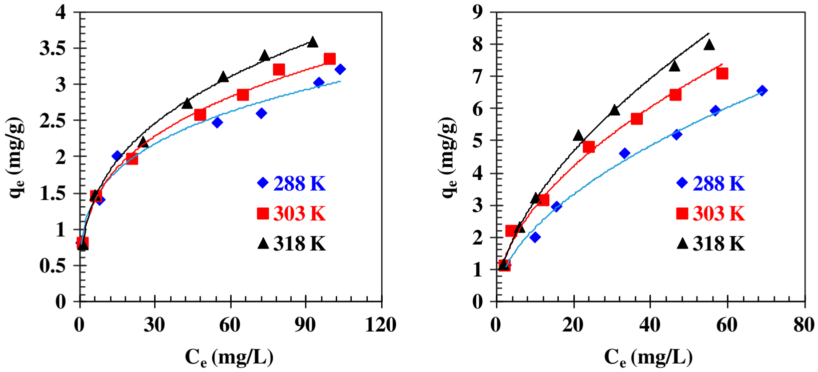

(a) RHA (b) GAC

Fig. 9. Equilibrium adsorption isotherms at different temperatures for BPA removal by RHA and GAC.

the solution at equilibrium at any constant temperature is termed adsorption isotherm [27]. Langmuir isotherm model assumes monolayer adsorption with homogeneous surface energy and no transmigration of solute. Freundlich isotherm model is applicable for heterogeneous surface. It assumes that each site has different bond energy and that the sites having stronger bond energy are occupied first [28]. Temkin isotherm contains a factor that explicitly takes into account the interaction between adsorbate and adsorbent. In this model, it is assumed that the decrease in heat of adsorption of molecule is linear with coverage and adsorption is characterized by uniform distribution of binding energy [29].

Values of parameters for different isotherm models namely Langmuir, Freundlich, and Temkin were evaluated and are tabulated in Table 2 along with the R^2 values at different temperatures. For Langmuir isotherm, the increase in the value of parameters (Q and b) with increase in temperature confirms the endothermic nature of the process. From Table 2, it can be observed that the values of $1/n$ for Freundlich isotherm is less than 1 at all temperature as well as for both the adsorbents, hence adsorption of BPA is favorable on both these adsorbents. The optimum adsorption capacity of GAC was found to be greater than RHA. This may be due to the higher surface area of GAC.

3.7. Estimation of thermodynamics parameters

Following equation was used for determining thermodynamics parameters [30]:

$$\ln K_{\text{ads}} = \frac{\Delta G^\circ}{RT} = \frac{\Delta S^\circ}{R} - \frac{\Delta H^\circ}{R}\frac{1}{T} \tag{7}$$

where ΔG° is free energy change (kJ/mol), R is universal gas constant (8.314 J/mol K), T is the temperature (K), and K_{ads} is the equilibrium constant for BPA between the solution and the adsorbent surface, ΔH° is the change on enthalpy (kJ/mol), ΔS° is the change in entropy (kJ/mol K). K_{ads} was evaluated from the intercept of $\ln(q_e\ /C_e)$ vs. q_e plot [31]. ΔH° was calculated from the slope of plot between $\ln K_{\text{ads}}$ and $(1/T)$. Values of all parameter are listed in Table 3. ΔG° values are negative indicating that the adsorption process led to a decrease in ΔG° and that the adsorption process is feasible and spontaneous [32]. Generally, the value of ΔG° is between −20 and 0 kJ/mol for physisorption; and in the range of −80 to −400 kJ/mol for chemisorption [32,33]. Most of the ΔG° values lie between −20 and 0 kJ/ mol indicating that the adsorption of BPA onto RHA and GAC is physical in nature. Positive values of ΔH° indicate the endothermic nature of BPA adsorption onto GAC and RHA. Solid/liquid and adsorption process completes in two steps: first step involves desorption of previously adsorbed water molecules and in the second step, adsorbate species adsorb on the adsorbent. The competition process required displacement of water molecule by BPA molecule. Energy is required for completion of this process due to which this adsorption of BPA becomes endothermic. In physiosorption, the bond between adsorbent and adsorbate is van der Walls interaction and ΔH° is typically in the range of 5–10 kJ/mol for liquid phase adsorption. In case of chemisorption, a chemical bond is formed between adsorbate molecules and the surface; and the chemisorption energy is, generally, in the range of 30–70 kJ/mol [34]. Values given in Table 3 indicate that adsorption for BPA onto RHA and GAC is by physical adsorption [35]. The positive value of ΔS° suggests increased randomness at the solid/solution interface with some structural

Table 2
Isotherm parameters for the removal of Bisphenol-A by RHA (t = 3 h, m = 30 g/L) and GAC (t = 3 h, m = 20 g/L)

		RHA			GAC		
Isotherms	Parameters	288	303	318	288	303	318
Langmuir $q_e = \frac{Q_0 b C_e}{1+bC_e}$	Q_0 (mg/g)	8.6655	8.7183	10.548	3.1420	3.5360	3.8446
	b (l/mg)	0.0362	0.0598	0.0496	0.0876	0.0922	0.0884
	R^2	0.947	0.9751	0.976	0.9594	0.9777	0.9755
Freundlich $q_e = K_F C_e^{1/n}$	K_F (mg/g)/(mg/L)$^{1/n}$	0.6528	0.8772	0.8519	0.8497	0.8147	0.7968
	$1/n$	0.5422	0.5225	0.5689	0.2589	0.3040	0.3322
	R^2	0.9908	0.9742	0.9971	0.9789	0.9976	0.9974
Temkin $q_e = B_T \ln (K_T C_e)$	B_T	1.6605	1.7533	2.0462	0.452	0.542	0.6169
	K_T (l/mg)	0.5222	0.7559	0.6767	5.843	3.1751	2.5030
	R^2	0.9274	0.9686	0.9506	0.9440	0.9963	0.9505

Table 3
Thermodynamic parameter for adsorption of Bisphenol-A by RHA (t = 3 h, m = 30 g/L) and GAC (t = 2 h, m = 20 g/L)

	K_{ads}	ΔG° (kJ/mol)	ΔH° (kJ/mol)	ΔS° (J/mol K)	K_{ads}	ΔG° (kJ/mol)	ΔH° (kJ/mol)	ΔS° (J/mol K)
Temperature (K)	BPA-RHA system				BPA-GAC system			
288	6.77	−4.58	0.3356	21.38	6.07	−4.32	4.032	29.6
303	6.72	−4.80			6.60	−4.75		
318	6.81	−5.02			6.62	−5.18		

changes in the adsorbate and the adsorbents. It also indicates an affinity of the adsorbents toward the BPA [36]. Positive ΔS° values also correspond to an increase in the degree of freedom of the adsorbed BPA species [37].

4. Conclusion

Present work reported removal of BPA from aqueous solution by adsorption process using low-cost RHA and high-cost GAC as adsorbents. Optimized condition for a solution containing 100 mg/L of BPA was: adsorbent dose = 30 g/L for RHA and 20 g/L for GAC; and time = 3 h for RHA and 2 h for GAC at natural pH of the solution. At optimized condition, the removal efficiency of BPA onto RHA and GAC was found to be 73.2% and 94%, respectively. Pseudo-second-order model best fitted the adsorption kinetic data for BPA removal onto RHA and GAC. Adsorption capacity of GAC was found to be better than that of RHA for BPA removal. Freundlich and Temkin model best represented the isotherm models for RHA and GAC, respectively. Adsorption of BPA onto GAC and RHA was endothermic and physical in nature.

References

[1] Q. Sui, J. Huang, Y. Liu, X. Chang, G. Ji, S. Deng, T. Xie, G. Yu, Rapid removal of bisphenol A on highly ordered mesoporous carbon, J. Environ. Sci. 23(2) (2011) 177–182.

[2] G. Xiao, L. Fu, A. Li, Enhanced adsorption of bisphenol A from water by acetylaniline modified hyper-cross-linked polymeric adsorbent: Effect of the cross-linked bridge, Chem. Eng. J. 191 (2012) 171–176.

[3] F. Cao, P. Bai, H. Li, Y. Ma, X. Deng, C. Zhao, Preparation of polyethersulfone–organophilic montmorillonite hybrid particles for the removal of bisphenol A, J. Hazard. Mater. 162 (2009) 791–798.

[4] G. Zeng, C. Zhang, G. Huang, J. Yu, Q. Wang, J. Li, B. Xi, H. Liu, Adsorption behaviour of bisphenol A on sediments in Xiangjiang River, Central-south China, Chemosphere 65 (2006) 1490–1499.

[5] A. Nakanishi, M. Tamai, N. Kawasaki, T. Nakamura, S. Tanada, Adsorption characteristics of bisphenol A onto carbonaceous materials produced from wood chips as organic waste, J. Colloid Interf. Sci. 252 (2002) 393–396.

[6] J. Fan, W. Yang, A. Li, Adsorption of phenol, bisphenol A and nonylphenol ethoxylates onto hypercrosslinked and aminated adsorbents, React. Funct. Polymers. 71 (2011) 994–1000.

[7] M. Clara, B. Strenn, E. Saracevic, N. Kreuzinger, Adsorption of bisphenol-A, 17β-estradiole and 17α-ethinylestradiole to sewage sludge, Chemosphere 56 (2004) 843–851.

[8] W. Su-Hua, D. Bing-zhi, H. Yu, Adsorption of bisphenol A by polysulphone membrane, Desalination 253 (2010) 22–29.

[9] K.K.H. Choy, G. McKay, J.F. Porter, Sorption of acid dyes from effluents using activated carbon, Resource Conser. Recycl. 27 (1999) 57–71.

[10] V.C. Srivastava, I.D. Mall, I.M. Mishra, Characterization of mesoporous rice husk ash (RHA) and adsorption kinetics of metal ions from aqueous solution onto RHA, J. Hazard. Mater. 134 (2006) 257–267.

[11] W. Nakbanpote, P. Thiravetyan, C. Kalambaheti, Preconcentration of gold by rice husk ash, Minerals Eng. 13(4) (2000) 391–400.

[12] V. Mane, I.D. Mall, V.C. Srivastava, Kinetic and equilibrium isotherm studies for the adsorptive removal of Brilliant Green dye from aqueous solution by rice husk ash, J. Environ. Manage. 84 (2007) 390–400.

[13] U.R. Lakshmi, V.C. Srivastava, I.D. Mall, D.H. Lataye, Rice husk ash as an effective adsorbent: Evaluation of adsorptive characteristics for Indigo Carmine dye, J. Environ. Manage. 90 (2009) 710–720.

[14] Y.Z. Wen, S.P. Tong, K.F. Zheng, L.W. Wang, J.Z. Lv, J. Lin, Removal of terephthalic acid in alkalized wastewater by ferric chloride, J. Hazard. Mater. 138(1) (2006) 169–172.

[15] S.R. Kamath, A. Proctor, Silica gel from rice hull ash: Preparation and characterization, Cereal Chem. 75 (1998) 484–487.

[16] M.M. Abou-Mesalam, Sorption kinetics of copper, zinc, cadmium and nickel ions on synthesized silico-antimonate ion exchanger, Colloid Surf., A 225 (2003) 85–94.

[17] M.M. Dávila-Jiménez, M.P. Elizalde-González, A.A. Peláez-Cid, Adsorption interaction between natural adsorbents and textile dyes in aqueous solution, Colloid Surf., A 254 (2005) 107–114.

[18] S. Ricordel, S. Taha, I. Cisse, G. Dorange, Heavy metals removal by adsorption onto peanut husks carbon: Characterization, kinetic study and modeling, Sep. Purif. Technol. 24 (2001) 389–401.

[19] M.S. Rauthula, V.C. Srivastava, Studies on adsorption/desorption of nitrobenzene and humic acid onto/from activated carbon, Chem. Eng. J. 168 (2011) 35–43.

[20] D. Rameshraja, V.C. Srivastava, J.P. Kushwaha, I.D. Mall, Quinoline adsorption onto granular activated carbon and bagasse fly ash, Chem. Eng. J. 181–182 (2012) 343–351.

[21] J.P. Chen, L. Wang, Characterization of metal adsorption kinetic properties in batch and fixed-bed reactors, Chemosphere 54 (2004) 397–404.

[22] Y.S. Ho, G. McKay, Pseudo-second order model for sorption processes, Process Biochem. 34 (1999) 451–465.

[23] W.H. Cheung, Y.S. Szeto, G. McKay, Intraparticle diffusion processes during acid dye adsorption onto chitosan, Bioresource Technol. 98 (2007) 2897–2904.

[24] W.J. Weber, J.C. Morris, Kinetics of adsorption on carbon from solution, J. Sanit. Eng. Div, Am. Soc. Civil Eng. 89 (1963) 31–59.

[25] J. Crank, The Mathematics of Diffusion, Oxford Clarendon Press, London, 1965.

[26] K.V. Kumar, S. Sivanesan, Comparison of linear and non-linear method in estimating the sorption isotherm parameters for safranin onto activated carbon, J. Hazard. Mater. B 123 (2005) 288–292.

[27] A.J. Jadhav, V.C. Srivastava, Adsorbed solution theory based modeling of binary adsorption of nitrobenzene, aniline and phenol onto granulated activated carbon, Chem. Eng. J. 229 (2013) 450–459.

[28] F. Haghseresht, G. Lu, Adsorption characteristics of phenolic compounds onto coal-reject-derived adsorbents, Energy Fuels 12 (1998) 1100–1107.

[29] M.I. Temkin, V. Pyzhev, Kinetics of ammonia synthesis on promoted iron catalysts, Acta. Physicochimica. URSS 12 (1940) 327–356.

[30] J.M. Smith, H.C. van Ness, M.M. Abbott. Introduction to Chemical Engineering Thermodynamics, fourth ed., McGraw-Hill, Singapore, 1987.

[31] V.C. Srivastava, I.D. Mall, I.M. Mishra, Adsorption thermodynamics and isosteric heat of adsorption of toxic metal ions onto bagasse fly ash (BFA) and rice husk ash (RHA), Chem. Eng. J. 132 (2007) 267–278.

[32] E. Sabah, M. Çinar, M.S. Çelik, Decolorization of vegetable oils: Adsorption mechanism of β-carotene on acid-activated sepiolite, Food Chem. 100 (2007) 1661–1668.

[33] S.D. Faust, O.M. Aly, Adsorption Processes for Water Treatment, Butterworths Publishers, Boston, 1987, pp. 108–113.

[34] D. Murzin, T. Salami, Chemical Kinetics, Elsevier, Amsterdam, 2005.

[35] C. Jianguo, L. Aimin, S. Hongyan, F. Zhenghao, L. Chao, Z. Quanxing, Equilibrium and kinetic studies on the adsorption of aniline compounds from aqueous phase onto bifunctional polymeric adsorbent with sulfonic groups, Chemosphere 61 (2005) 502–509.

[36] S. Suresh, V.C. Srivastava, I.M. Mishra, Isotherm, thermodynamics, desorption, and disposal study for the adsorption of catechol and resorcinol onto granular activated carbon, J. Chem. Eng. Data 56 (2011) 811–818.

[37] C. Raymon, Chemistry: Thermodynamic, McGraw-Hill, Boston, MA, 1998.